# Atmospheric Pressure Tornado Plasma Jet of Polydopamine Coating on Graphite Felt for Improving Electrochemical Performance in Vanadium Redox Flow Batteries

Song-Yu Chen [1], Yu-Lin Kuo [1,*], Yao-Ming Wang [2], Wei-Mau Hsu [2], Tzu-Hsuan Chien [1], Chiu-Feng Lin [2,3], Cheng-Hsien Kuo [4], Akitoshi Okino [5] and Tai-Chin Chiang [6]

[1] Department of Mechanical Engineering, National Taiwan University of Science and Technology, No.43, Section 4, Keelung Road, Taipei 10607, Taiwan; D10803004@gapps.ntust.edu.tw (S.-Y.C.); a0970001411@gmail.com (T.-H.C.)

[2] Metal Industries Research & Development Centre, Kaohsiung 81160, Taiwan; yawang@mail.mirdc.org.tw (Y.-M.W.); weimau@mail.mirdc.org.tw (W.-M.H.); chiufeng@mail.nirdc.org.tw (C.-F.L.)

[3] Department of Vehicle Engineering, National Pingtung University of Science and Technology, Neipu, Pingtung 91207, Taiwan

[4] Department of Mold and Die Engineering, National Kaohsiung University of Science and Technology, No.415, Jiangong Road, Kaohsiung 80778, Taiwan; chuckkuo@nkust.edu.tw

[5] Laboratory for Future Interdisciplinary Research of Science and Technology, Tokyo Institute of Technology, Yokohama 226-8502, Japan; aokino@es.titech.ac.jp

[6] Global Development Engineering Program, National Taiwan University of Science and Technology, Taipei 10607, Taiwan; tcc@mail.ntust.edu.tw

* Correspondence: ylkuo@mail.ntust.edu.tw; Tel.: +886-2-27376784; Fax: +886-2-27376460

**Abstract:** The intrinsic hydrophobicity of graphite felt (GF) is typically altered for the purpose of the surface wettability and providing active sites for the enhancement of electrochemical performance. In this work, commercial GF is used as the electrodes. The GF electrode with a coated-polydopamine catalyst is achieved to enhance the electrocatalytic activity of GF for the redox reaction of vanadium ions in vanadium redox flow battery (VRFB). Materials characteristics proved that a facile coating via atmospheric pressure plasma jet (APPJ) to alter the surface superhydrophilicity and to deposit polydopamine on GF for providing the more active sites is feasibly achieved. Due to the synergistic effects of the presence of more active sites on the superhydrophilic surface of modified electrodes, the electrochemical performance toward $VO^{2+}/VO_2^+$ reaction was evidently improved. We believed that using the APPJ technique as a coating method for electrocatalyst preparation offers the oxygen-containing functional groups on the substrate surface on giving a hydrogen bonding with the grafted functional polymeric materials.

**Keywords:** vanadium redox flow battery (VRFB); polydopamine; graphite felt (GF); electrode; atmospheric pressure plasma jet (APPJ)

## 1. Introduction

Various renewable energy sources such as wind power systems, geothermal energy systems, and solar cells have attracted considerable attention due to the greenhouse effect and environmental hazards of fossil fuels. However, the intermittent and unpredictable of electricity generation limits these renewable energy generators as an alternative to fossil fuel. To mitigate this risk, the development of various energy storage systems (ESS) technologies with different mechanisms was proposed elsewhere [1,2]. Among these, the utilization of a large-scale ESS is leading to rapid development. A high market share of ESS is expected as the key technology to balance and shift the energy. In this regard, vanadium redox flow battery (VRFB) is one of the possible large-scale energy storage system that contributed to a high storage capacity, fast response time, low maintenance

cost, and long lifetime (over 10,000 cycles) [3–6]. The VRFB system is based on changing the oxidation of vanadium species especially in different redox couples (Cathode: ($VO^{2+}/VO_2^+$), Anode: ($V^{2+}/V^{3+}$)) [7]. The vanadium electrolytes are based on aqueous acidic media circulation through graphite felt (GF) electrode with high surface area and chemical stability, which are necessary to produce effective ion exchange and high acid resistance during the electrochemical operations [8–10]. However, GF is a carbon-based material with intrinsic hydrophobicity and poor wettability. The limitations of GF make it not suitable for the VRFB electrolyte solution. Several metal or metal oxides catalysts including Pt, Pd, Ir, Bi, $CuPt_3$, $Nb_2O_5$ and $PbO_2$ are able to improve the electrochemical performance of electrodes [11]. Due to the noble metal, non-metallic functionalization and complex preparation processes of catalyst materials there is limited market application of the VRFB system [12,13]. Furthermore, the current loading and flowing electrolyte in VRFB system causes the poor adhesion of catalysts on the electrodes. To mitigate the issues of metal-based catalysts, N-doped carbon materials have been shown to improve the electrochemical performance of the VRFB system [14–16]. Several preparation strategies have been developed for synthesizing polydopamine as the nitrogen source for modifying GF. Lee et al. reported that nitrogen-doped GF prepared via deposition of different thin film of polydopamine followed by pyrolysis in an argon atmospheric [15]. Youn et al. reported producing nitrogen-functionalized GF by ultra-sonication assisted self-polymerization and pyrolysis of dopamine [17]. These reported studies mainly demonstrated the polydopamine coating on GF and subsequent heat treatment to prepare nitrogen-functionalized GF for improving the performance of a VRFB system [15,17,18]. However, the proposed methods for functionalization on the surface are complicated and require longer processing time. Ji et al. firstly proved that the polydopamine coating on GF evidently enhanced energy efficiency in a VRFB single cell [19]. Hence, our maturely designed and environmentally friendly process based on the surface treatment and coating technologies via an atmospheric pressure plasma jet (APPJ) system were reported on the previous studies, such as the enhanced abrasion resistance of an anti-fingerprint coating on plated-Cr/brass substrates, a modified $LiFePO_4$ electrode for improved high-temperature performance in Li-ion batteries (LIBs), and lanthanum strontium manganite (LSM) as a cathode layer in solid oxide fuel cell (SOFC) [20,21]. This work focused on the development of APPJ technique using argon plasma to directly deposit polydopamine on GF substrates to achieve an excellent electrochemical performance in a VRFB system.

## 2. Results and Discussion

The APPJ system used in this study is equipped with a mass flow controller to control the flow rate of Ar gas as the working gas. In the initiation step of homogeneous plasma generation, Ar gas under the electric field received the kinetic energy from the elastic collisions of molecules, in which the momentum is conserved. Subsequently, the dissociation and the ionization of Ar gas proceed via inelastic collisions, in which the energy is transferred from the electrons under the applied electric field to Ar gas [22,23]. The formation of total plasma species under ambient pressure in an Ar-APPJ system is detected by OES, as shown in Figure 1a. The strong spectral lines in Ar emission spectrum are denoted as the transitions from 2p to 1s locating at the range of 690–900 nm, which correspond with the NIST Atomic Spectra Database [24]. Apart from the observed Ar emission lines, however, some significant peaks corresponded to the atomic oxygen (OI) at 777.1 nm and 840.6 nm, $N_2$ species at 310–440 nm ($N_2$ bands), and OH band at 309 nm from the ambient air were detected, respectively. Due to the high flow rate of Ar working gas (35 slm) in APPJ system, the high flux plasma density which ion-bombards on the substrate materials contributes the surface modification process accompanying the accumulated heat. In Figure 1b, the appearance of a visible tornado plasma flame is purple and sharp, with the flame length around 5 mm working distance. The gas temperature in an Ar-APPJ system is first measured using a thermometer with the k-type thermocouple covered with the quartz tube below the plasma head of 0 and 5 mm working distance. The temperatures

with different distances reached the maximum values of 73 °C (0 mm) and 57 °C (5 mm) within 120 s. As the plasma was turned off, the system was cooled down with argon to reach room temperature for a further 30 s.
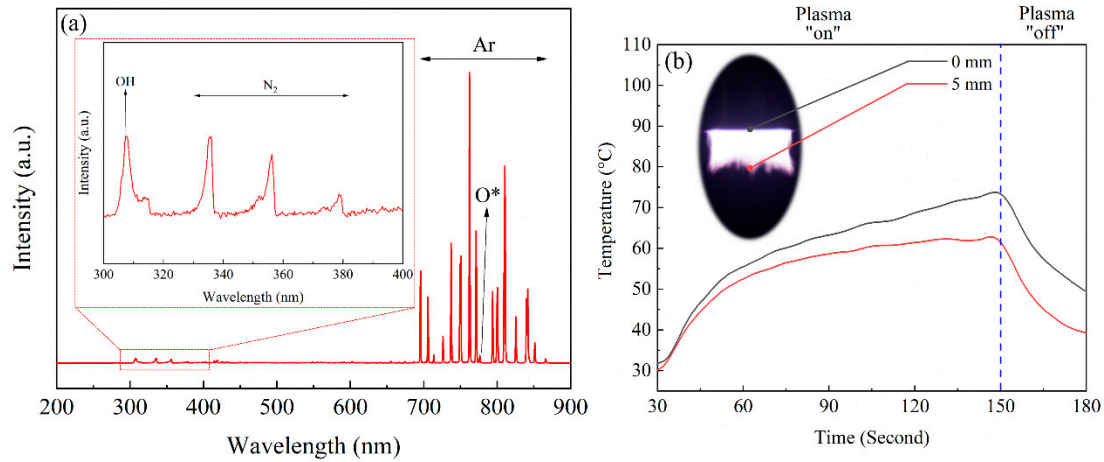


**Figure 1.** (**a**) OES obtained from Ar-APPJ process, (**b**) argon plasma with a plume length of 5 cm and gas temperature.

PAN-based GF with high conductivity, high purity, and chemical resistance in acid solution is widely used as the electrode in VRFB system. In order to understand the stability of GF under the plasma treatment, a TGA test was implemented, as shown in Figure 2. A small weight gain from 25 °C to 75 °C is contributed by the gas absorption of the air on the GF sample and maintains thermally stability up to approximately 650 °C. A significant weight loss over 650 °C is contributed from the oxidation of GF by air gas to form $CO_2$ gas which is released into the environment. In this study, the Ar-APPJ system is also denoted as cold atmospheric plasma, in which the low gas temperature for functionalization and coating processes of polydopamine on GF substrates was feasibly achieved.
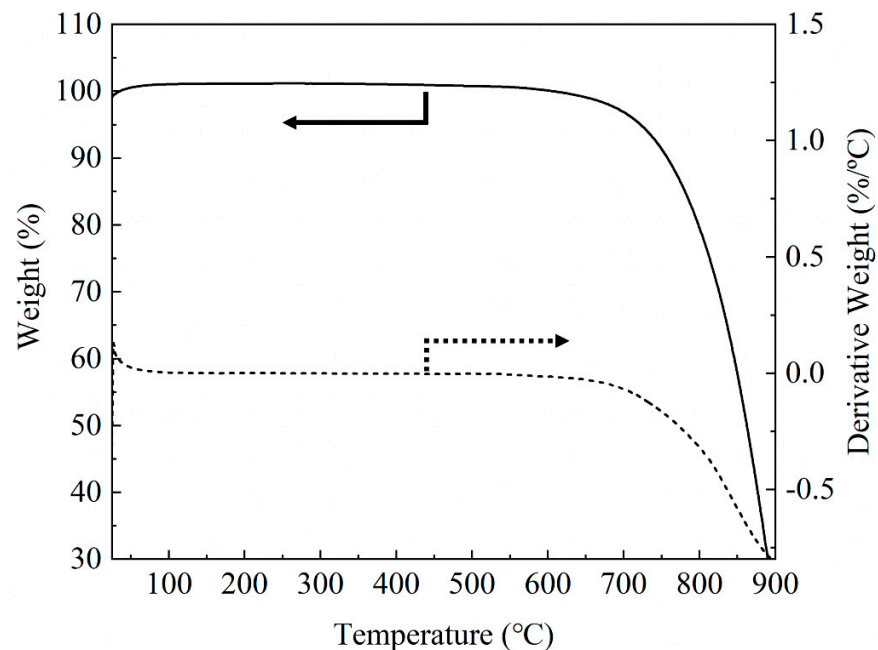


**Figure 2.** TGA/DTG curves of pristine GF.

The GF electrode composed of the interlinked fibers in the VRFB system requires a high porosity with a large surface area to provide absorption well for the electrolyte solution to exchange oxidation of the vanadium ions [25]. The morphologies of pristine GF

fibers along the axial direction was observed, as shown in Figure 3a,b. The fiber surface is smooth without any visible defects. In Figure 3c,d, the contact angles of DI water and VRFB electrolyte solution on pristine GF are 135.7 ° and 127.9 °, indicating the intrinsically hydrophobic surface, which was evidently proved by dropping the sample into the VRFB electrolyte solution. The pristine GF still floats on the surface of the aqueous solution, referring to a poor wettability in the VRFB system (Figure 3e). Wu et al. reported that air bubbles on the hydrophobic GF surface were observed, which resulted in in the unstable electrochemical stability during the charging/discharging processes in a VFRB system [26]. Previous studies were reported to demonstrate the improvement on the wettability and the activity of GF for the VRFB system [27–31].
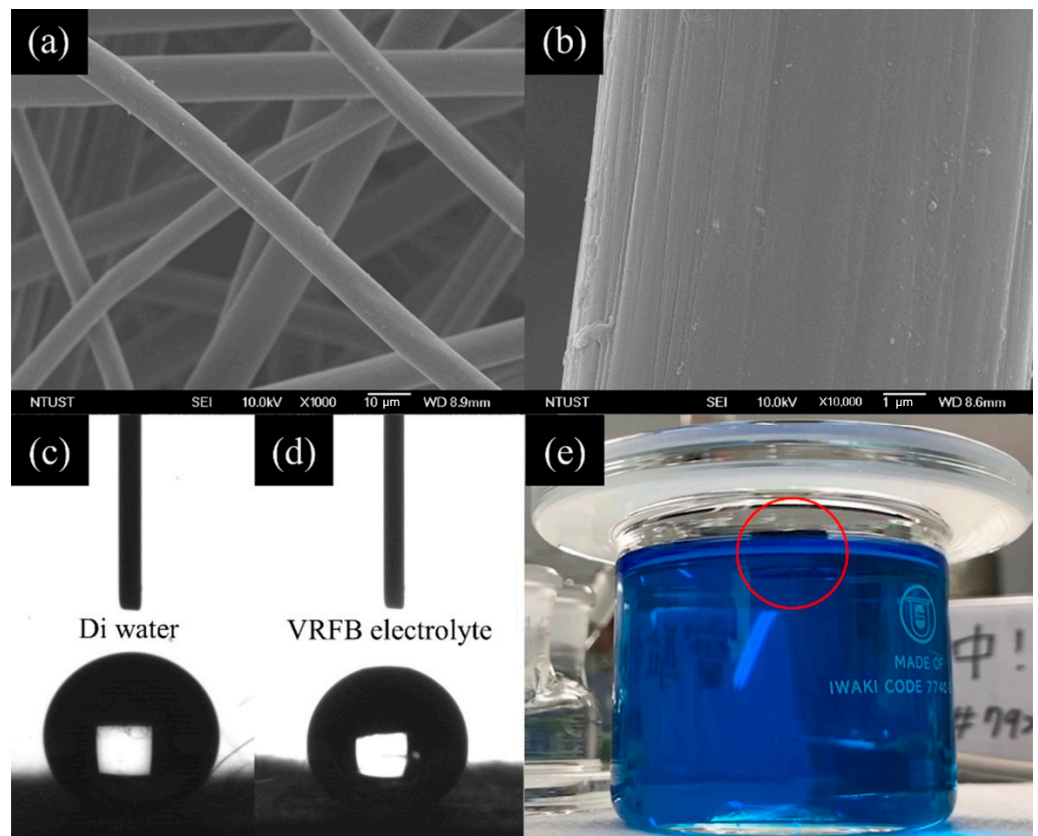


**Figure 3.** SEM images of pristine GF (**a**) × 1000 (**b**) ×10,000, and the contact angle measurements of pristine GF using (**c**) deionized water (**d**) VRFB electrolyte solution, and (**e**) a sinking test in VRFB electrolyte solution.

In Figure 4a,b, SEM images represent a portion of APPJ-coated polydopamine decorated onto the surface of the GF samples. In order to understand the wettability of APPJ-coated polydopamine on GF, the contact angles using deionized water and VRFB electrolyte solution were obtained, which also confirmed that the superhydrophilic properties on GF samples was visually sunk into the VRFB electrolyte solution (Figure 4c–e). We speculated that the enhancement of the wettability of APPJ-coated polydopamine on GF is mainly contributed by the functional groups of polydopamine. Therefore, the electrolyte utilization and the energy efficiency of the superhydrophilic GF surface in VRFB system are expected to be improved [27,29].
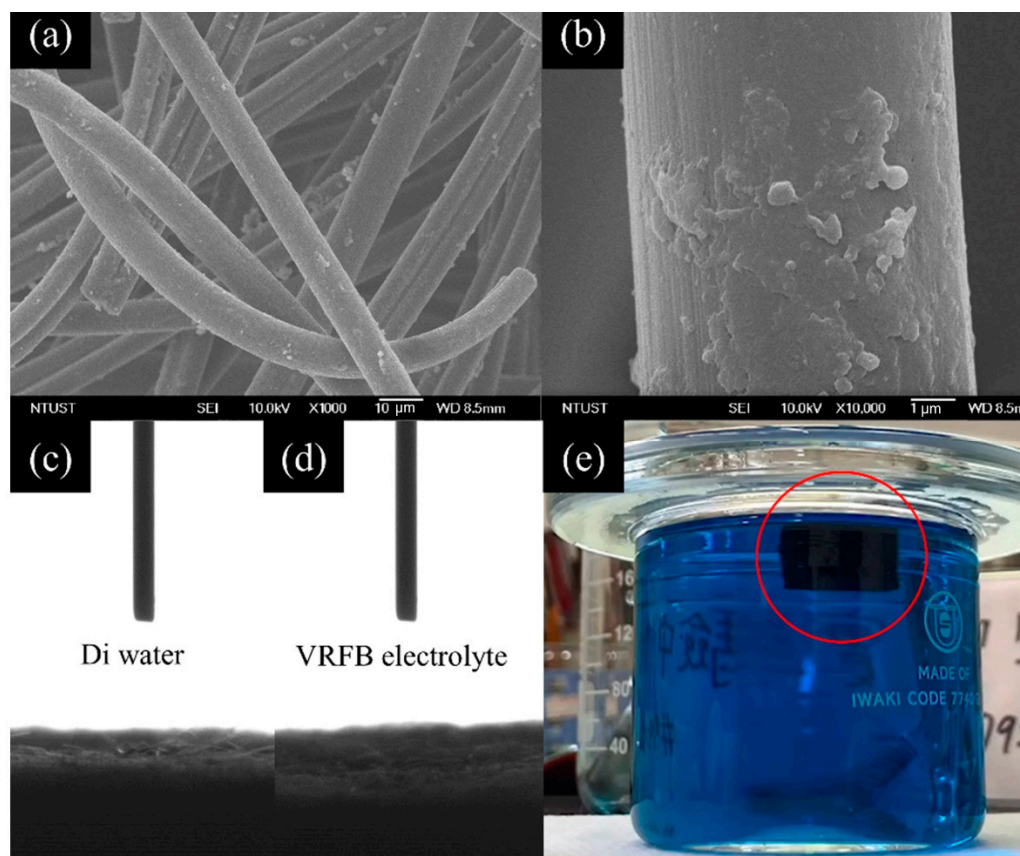
**Figure 4.** SEM images of APPJ-coated polydopamine on GF (**a**) ×1000 (**b**) ×10,000, and the contact angle measurements of pristine GF using (**c**) deionized water (**d**) VRFB electrolyte solution, and (**e**) a sinking test in VRFB electrolyte solution.

Raman spectroscopy (RS) was further performed to investigate the microstructure of the GF samples, as shown in Figure 5. Two significantly characteristic peaks located at the wavenumbers of 1346 and 1580 cm$^{-1}$ are attributed to the D and G bands, respectively. The D and G bands are corresponding to A1g symmetry which is associated with the sp$^3$ defect sites and the E2g symmetry of sp$^2$ domains, respectively [27,32,33]. The ratios of $I_D/I_G$ of pristine GF and APPJ-coated polydopamine on GF are 1.014 and 1.031, respectively. Hence, the larger the ratio of $I_D/I_G$ is, the more defect sites are obtained, indicating more vanadium ions involved in the electrochemical reactions in the VRFB system [32,34]. Moreover, the RS bands at 1060 cm$^{-1}$ (C-C-N stretching) and 1117 cm$^{-1}$ (NH twisting) are attributed to the characteristics of polydopamine coated by the APPJ system [35].

The chemical compositions of APPJ-coated polydopamine on GF surfaces were analyzed by XPS. In Figure 6, N1s spectrum is deconvoluted into two peaks assigned to the pyrrolic N and the pyridinic N*- O$^-$ belonging to the functional groups in polydopamine, which is composed of indole and dopamine units. Pyrrolic N in polydopamine provides the structure with defects due to its location at the edge of C layers. He et al. reported that the more defects existed in ploydopamine lead to the increase in the surface wettability and act as active sites for the electrochemical reactions [36]. The results of Raman spectra and XPS analysis are correspond to the findings of SEM images (Figure 4a,b) for the confirmation of the existence of polydopamine coating on GF. The contact angel measurement and immersion test in the VRFB electrolyte solution are proved to a higher wettability of APPJ-coated polydopamine on GF, as shown in Figure 4c–e.
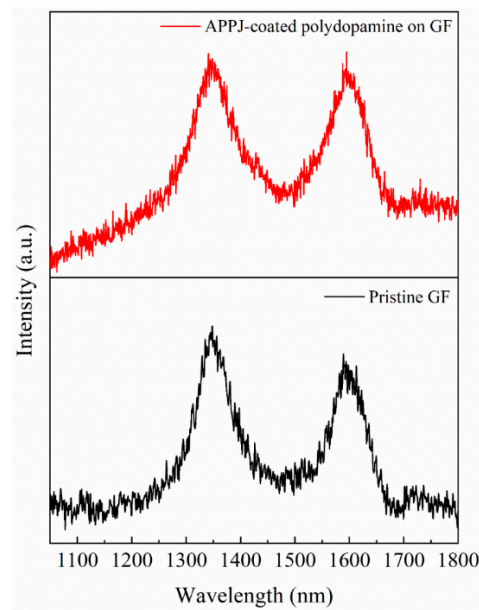
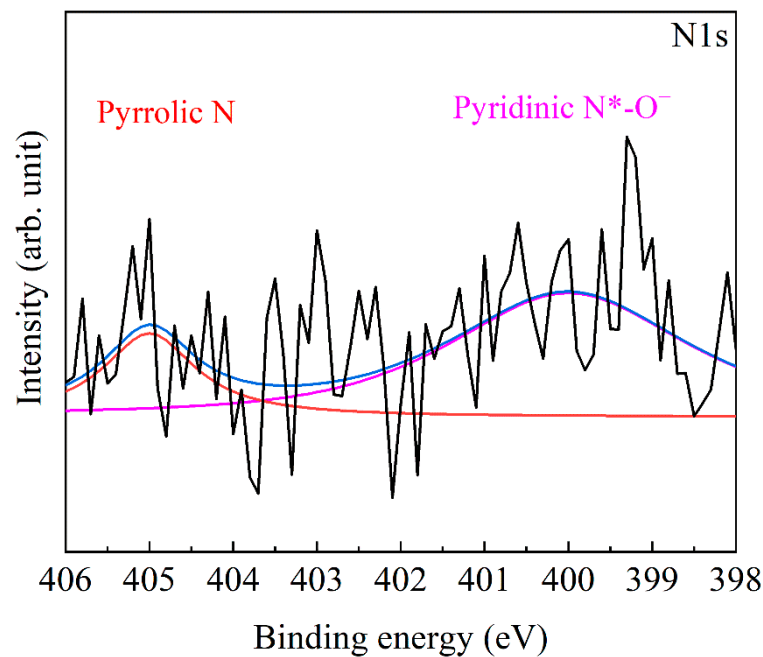**Figure 5.** Raman spectrum of pristine GF and APPJ-coated polydopamine on GF.



**Figure 6.** XPS spectrum of APPJ-coated polydopamine on GF.

CV tests were performed to understand the electrochemical activity of electrodes toward $VO^{2+}/VO_2^+$ redox reaction in 0.05 M $VOSO_4$ and 2 M $H_2SO_4$ solutions. The peak potential separation ($\Delta E_p = V_{pa} - V_{pc}$) and peak current densities ratio ($J_{pa}/J_{pc}$) of maximum peaks for the reversibility of the reaction and possess good symmetry at a scan rate of 5 mV/s [37]. In Figure 7, the $\Delta E_p$ value for APPJ-coated polydopamine on GF is 0.69 V, which is similar with the pristine GF ($\Delta E_p = 0.61$ V). The $J_{pa}/J_{pc}$ ratio of pristine GF is 1.71, while the value of APPJ-coated polydopamine on GF is decreased into 1.32. It is believed that the $J_{pa}/J_{pc}$ ratio is more equal to one, referring to the better reversibility of the redox reaction of vanadium ions in a VFRB system. The GF substrate soaked in the polydopamine solution was also used as the conventional method for the comparison. The $\Delta E_p$ value and the $J_{pa}/J_{pc}$ ratio are 1.63 V and 1.81, displaying a poor electrochemical performance in a VFRB system.
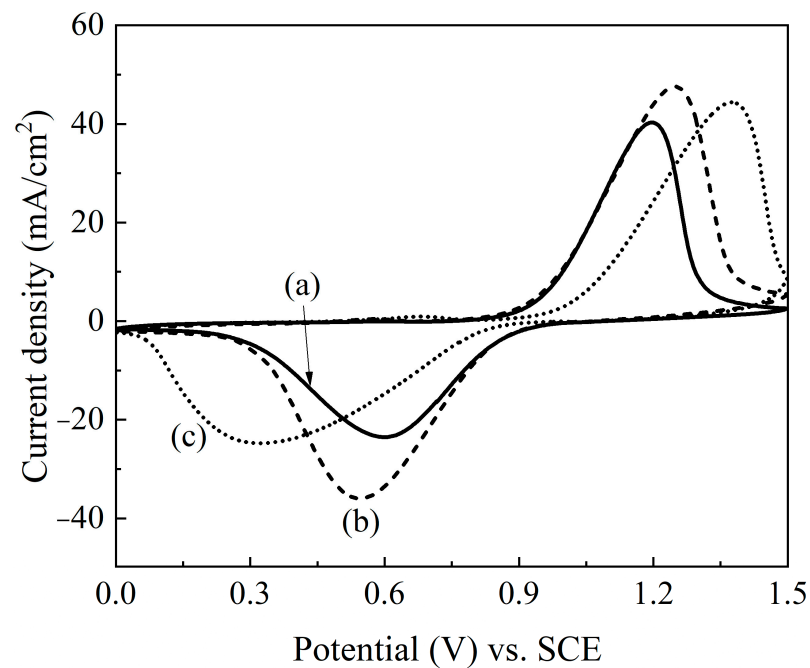
**Figure 7.** CV test curves of prepared electrodes at a scan rate of 5 mV/s, (**a**) pristine GF, (**b**) APPJ-coated polydopamine on GF, and (**c**) soaking GF in polydopamine solution.

To understand the catalytic effect of polydopamine coating on GF, a typical charge–discharge test using the VRFB single cell in 1.6 M $VOSO_4$ in a solution of 2.5 M $H_2SO_4$ was performed. The suitable potential window ranging from 0.7 to 1.6 V was implemented for the inhibition of side reactions, such as water electrolysis for producing $O_2$ and $H_2$ gases [38]. Figure 8a,b present the charge–discharge curves for electrodes at the current densities of 40 and 80 mA/cm$^2$. For the VRFB cell with direct coating of polydopamine on GF via the APPJ system, the prepared electrodes revealed the longer charge–discharge time and a lower charge voltage plateau, which are contributed from the synergistic effect of the superhydrophilic surface toward the VRFB electrolyte solution and pyrrolic N in polydopamine for producing more active sites for the $VO^{2+}/VO_2^+$ redox reaction [29,36,37,39].
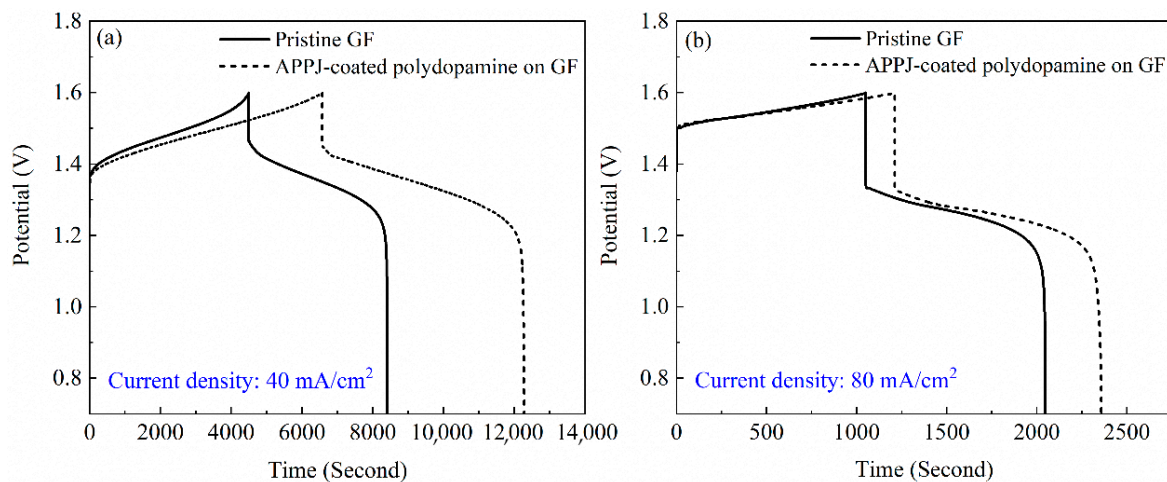


**Figure 8.** Charge–discharge curves of VRFB single cell using pristine GF and APPJ-coated polydopamine on GF as electrodes at a current density of (**a**) 40 mA/cm$^2$ and (**b**) 80 mA/cm$^2$.

Figure 9 shows the charge–discharge curves for the VRFB single cell with APPJ-coated polydopamine on GF surfaces electrodes at different current densities, and the corre-

sponding efficiencies including Columbic efficiency (CE), Voltage efficiency (VE), Energy efficiency (EE), are listed in Table 1. As increasing the current densities, CE apparently increased, while VE and EE dramatically decreased. The increasing trend on CE values with current densities is contributed from the reduced time of vanadium ion crossover through Nafion membranes [40,41]. However, at the higher charge–discharge rate in VRFB single, the decreases in VE and EE resulted from the increased overpotential caused by cell polarization [11,41].
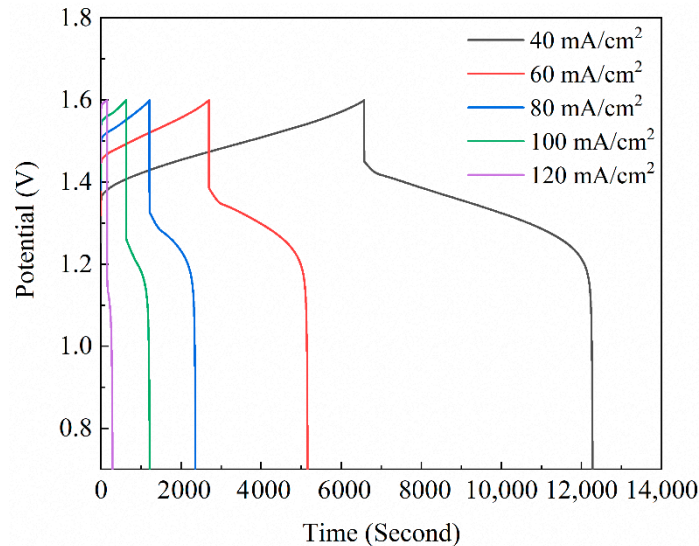


**Figure 9.** Efficiencies of the VRFB single cell with APPJ-coated polydopamine on GF at different current densities.

**Table 1.** Efficiencies of the VRFB single cell with APPJ-coated polydopamine on GF at different current densities of 40, 60, 80, 100 and 120 mA/cm$^2$.

| Current density (mA/cm$^2$) | CE (%) | VE (%) | EE (%) |
|---|---|---|---|
| 40 | 85.24 | 93.83 | 79.86 |
| 60 | 91.90 | 86.15 | 79.16 |
| 80 | 93.81 | 81.39 | 76.31 |
| 100 | 95.11 | 77.21 | 73.42 |
| 120 | 96.02 | 69.84 | 67.02 |

GF is a carbon-based material with intrinsic hydrophobicity and shows a poor energy efficiency in VRFB system. According to the experimental results mentioned above, surface treatment by argon plasma induced oxygen-containing functional groups on GF was achieved [42,43]. In Figure 10, we believed that the hydrogen bonding between the catechol group of polydopamine and oxygen-containing functional groups on GF was evidently occurred for a better interfacial bonding [44–46]. Integrating the wettability of GF for the electrochemical reaction of vanadium ions can be described for the generated triple phase boundary (TPB) among VRFB electrolyte solution, polydopamine catalyst, and GF. The pyrrolic-N species in polydopamine possessing the superhydrophilic properties facilitates the reaction of vanadium ions and donates electrons to the π-system, which is composed of HOMO and LUMO levels, leading to electrical conductivity [47,48]. According to the results outlined by Li et al., the higher diffusion coefficient of polydopamine and the lower charge transfer resistance of the VRFB single cell using polydopamine modified GF as the electrode. It possessed a smaller polarization value and a higher electrolyte utilization as compared with that of VRFB with blank GF [19].
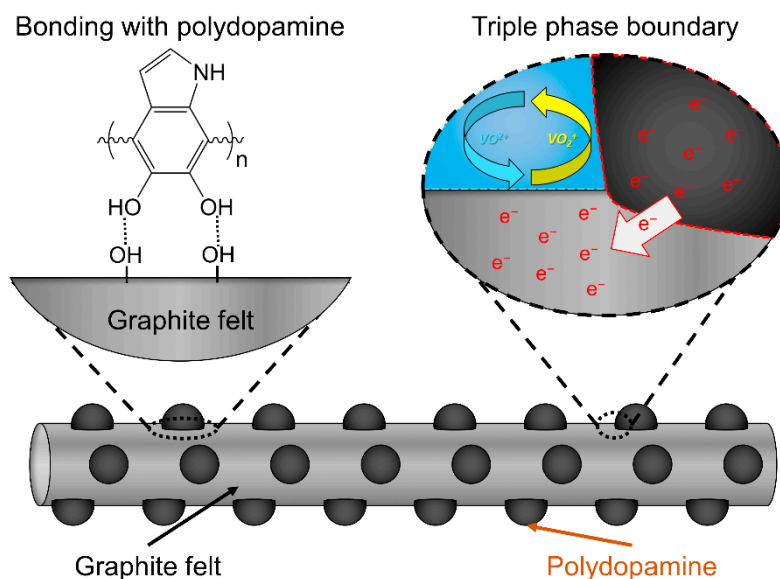
**Figure 10.** Mechanisms of synergistic effects on functionalization and coating processes of polydopamine on GF substrates by APPJ for enhancing the VRFB performance.

To achieve a higher electrochemical performance of GF in the VRFB system, research based on the surface treatment methods and deposition of heavy metals and metal oxide were widely discussed [11]. The energy efficiency of the VRFB with polydopamine modified GF was accordingly compared with various electrocatalysts reported in the previous studies as listed in Table 2. Our work shows polydopamine modified GF at a current density of 40 mA/cm$^2$ is 79.86%, which is higher than those of the previous studies that demonstrated electrocatalyst materials at a current density of 40 mA/cm$^2$ were < 75%. The EE of $MoO_2$/MSU-FC fabricated by Kwon et al. is 72.5% at a current density of 80 mA/cm$^2$, in which is apparently lower than this work. However, the previous studies for electrocatalyst coating require a long producing time with complicated processes involved. Furthermore, APPJ system offers the advantages of a rapid coating process and the ability to treat a large surface area of economical GF electrodes.

**Table 2.** Comparison of APPJ-coated polydopamine on GF as electrode materials with the literature.

| Catalyst/Electrode | Current Density (mA/cm$^2$) | Efficiency | | | Ref |
|---|---|---|---|---|---|
| | | CE (%) | VE (%) | EE (%) | |
| Pt-C/CF | 10 | 80.6 | 89.7 | 72.3 | [49] |
| Pt/MWNTs | 20 | 83.88 | 27.55 | 23.11 | [50] |
| Pt-C/sprayed GF | 40 | 87 | 84 | 71 | [51] |
| Ir/GF | 40 | 82 | 74.6 | 61.1 | [52] |
| $Mn_3O_4$/CF | 40 | 83.5 | 91 | 76 | [53] |
| $MoO_2$/MSU-FC | 80 | 91 | 79.7 | 72.5 | [54] |
| APPJ polydopamine coating/GF | 40 | 85.24 | 93.83 | 79.86 | This work |
| | 80 | 93.81 | 81.39 | 76.31 | |

## 3. Experimental

Commercial PAN-based GF (Model: GF065, thickness: 6.5 mm, base weight: 590 g/m$^2$, carbon content: 98.5%, CeTech Co., Ltd, Taichung, Taiwan) was applied in this research as the electrode in the VRFB system. Samples were cut into test strips of 50 mm × 50 mm squares as the pristine GF. Details of polydopmaine preparation by

self-polymerization of dopamine is highlighted in the previous study [17]. The chemicals, including tris-(hydroxymethtl)-aminomethane (99.8%, Scharlau, Barcelona, Spain), 3-hydroxytyramine hydrochloride (99%, Acros organics, Geel, Belgium), vanadyl (IV) sulfate hydrate (17–23% V, Acros organics, Geel, Belgium), and sulfuric acid (95–98%, Scharlau, Spain) were used in this work. All chemicals were analytical-reagent grade without further purification and directly used for the preparation of the chemical precursor.

We used the commercial tornado-type APPJ system (Click-SSV1, Click Sun Shine Corp., New Taipei City, Taiwan) for coating process, as depicted in Figure 11. It is equipped with a rotating jet head (tornado-type) by an AC power system, an atomizer for the chemical precursor delivery, and a moving stage for area scanning. The plasma is generated using argon as the working gas, which is supplied at a constant flow rate of 35 slm. The substrates were set on the moving stage with a nozzle-to-sample distance at 5 mm, and the parameter associated with plasma power and moving stage movement velocity were 500 W and 50 mm/s, respectively. An atomizer using the piezoelectric oscillator with a frequency of 2.45 MHz is used to generate the atomized polydopamine solution droplets, which was transferred by argon as the carrier gas at a constant flow rate of 15 sccm (See supplementary materials and video, Video S1). Prior to the polydopamine coating by the APPJ system, the GF substrates were washed with de-ionized water and ethyl alcohol three times.
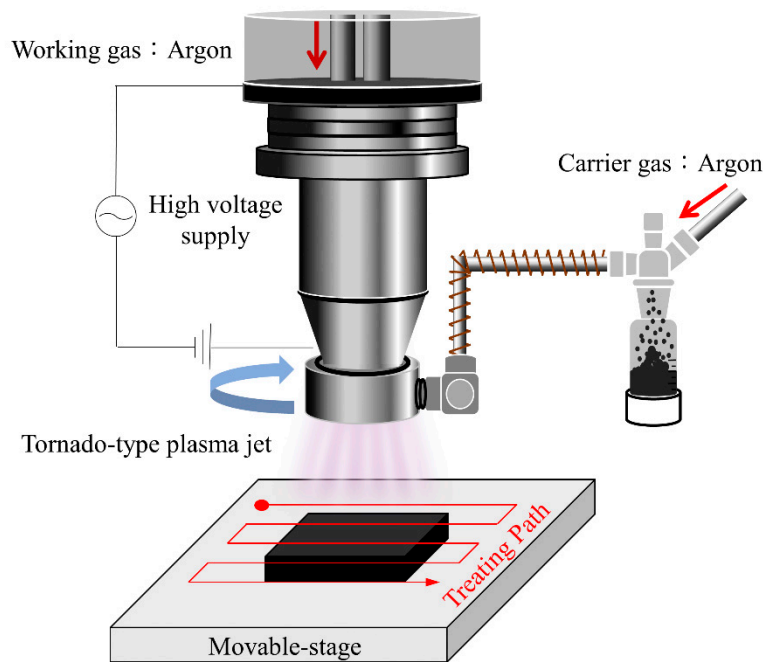


**Figure 11.** Schematic apparatus of the tornado-type atmospheric pressure plasma coating system.

The temperature was measured via TES-1370 thermometer with a k-type thermocouple of argon plasma plume, which will change with varying distance to the substrate. To characterize the formation of plasma species in plasma, optical emission spectroscopy (OES, Mars HS2000+, GIE Optoelectronics Inc., Taipei, Taiwan) measurements are presented. Furthermore, the measurement necessary conducts in the photon-less environment. Advances in characterization of GF via thermal gravimetric analysis (TGA, STA 449 F3 Jupiter ®, Netzsch Instruments, GmbH, Weimar / Thuringia, Germany) and different thermal gravimetric (DTG) were investigated when the sample was heated from 25 °C to 800 °C in an air atmospheric, to investigate weight gain or loss in the dissimilar temperature treatment process. Surface morphologies of each samples were obtained by a field emission scanning electron microscope (FE-SEM, JEOL, JSM 7900F, Tokyo, Japan) with an accelerating voltage of 15 kV. In order to evaluate the wettability and static contact angle were measured by contact angle equipment (Model 100SB, Sindatek Instrument Co., Ltd, Taipei, Taiwan) with sessile drops of a micro syringe (5 μl) on each sample to eliminate the effects of droplet size

and gravity. The change of structures of GF samples were proven by Raman spectroscopy (iHR550, Horiba, Kyoto, Japan) with 632 nm He-Ne laser as the excitation source and scanned at 350–4000 cm$^{-1}$. The surface compositions of each specimen were analyzed via X-ray photoelectron spectroscopy (XPS, Thermo Theta Probe, Thermo Fisher Scientific Inc., East Grinstead, UK). With X-ray source of the monochromatized Al-K$\alpha$ X-ray type (h$\nu$ = 1486.6 eV), peak positions were carefully calibrated with to the C1s graphitic peak position at 284.5 eV from the adventitious hydrocarbon contamination. Peak spectra were deconvoluted using the Shirley background function and an asymmetrical Lorentzian-Gaussian peak shape by software (XPS peak 4.1).

GF specimens were characterized with electrochemistry using cyclic voltammetry (CV) measurements which was conducted in a three-electrode cell with an electrochemical workstation (VSP-300, Bio-Logic, Claix, France) in the electrolyte of 0.05 M VOSO$_4$ + 2 M H$_2$SO$_4$ and purged with nitrogen at an ambient temperature. The GF samples were placed in the customization PTFE holder as a working electrode; a Pt wire and saturated calomel electrode (SCE) were used as the counter and reference electrodes, respectively. The scanning potential range of CV was limited from 0 V to 1.5 V versus SCE, and the scanning rate was 5 mV/s.

A VRFB single cell test was performed using two pieces of pristine GF and APPJ-coated polydopamine on GF with an active area of 25 cm$^2$ (5.0 cm $\times$ 5.0 cm) as the electrode. Graphite plates with a flow field and proton exchange membrane (Nafion 117, Du-Pont, Wilmington, DE, USA) were used as the current collector and separator, respectively. Rubber was utilized as the washers to seal the single cell. The dosing pumps (QG400Q2CKC, Consortech corporation, Taipei, Taiwan) with the flow rate of the electrolyte maintained at 30 mL/min. The initial electrolyte was 50 mL with concentrations at both sides of 1.6 M VOSO$_4$ in a solution of 2.5 M H$_2$SO$_4$. Finally, the potential of charge and discharge profiles of the VRFB were evaluated between 1.6 V and 0.7 V at current densities of 40 mA/cm$^2$, 60 mA/cm$^2$, 80 mA/cm$^2$, 100 mA/cm$^2$ and 120 mA/cm$^2$.

## 4. Conclusions

To enhance the electrocatalytic activity of GF electrodes towards the redox reaction of vanadium ions, polydopamine was easily coated on the surface of the electrode using an APPJ system. APPJ-coated polydopamine on GF was demonstrated to have a superhydrophilic surface via the hydrogen bonding between the catechol group of polydopamine and generated oxygen-containing functional groups on GF surface, in which it was visually sunk into the VRFB electrolyte solution [44–46]. According to the CV and charge–discharge tests, better performance of the modified GF electrodes was achieved, contributing from the superhydrophilic surface and more active sites appeared on polydopamine and GF. This finding is due to the synergistic effects related to the presence of more active sites on the superhydrophilic surface of electrodes, indicating the APPJ-coated polydopamine could make the GF provide a considerable electrochemical behavior to facilitate the VO$_2^+$/VO$^{2+}$ redox reaction in the VRFB system. Hence, CE, VE, and EE of VRFBs with polydopamine modified GF are 93.81%, 81.39% and 76.31% at current density 80 mA/cm$^2$, which is much higher than other reported electrodes. Furthermore, we also believe that using the APPJ technique is suitable as a coating method for electrocatalyst preparation to improve the electrochemical performance of the VRFB system.

**Conflicts of Interest:** The authors declare no conflict of interest.

## References

1. Noh, C.; Moon, S.; Chung, Y.; Kwon, Y. Chelating functional group attached to carbon nanotubes prepared for performance enhancement of vanadium redox flow battery. *J. Mater. Chem. A* **2017**, *5*, 21334–21342. [CrossRef]
2. Lee, H.J.; Choi, N.H.; Kim, H. Analysis of concentration polarization using UV-visible spectrophotometry in a vanadium redox flow battery. *J. Electrochem. Soc.* **2014**, *161*, A1291. [CrossRef]
3. Chang, T.-C.; Zhang, J.-P.; Fuh, Y.-K. Electrical, mechanical and morphological properties of compressed carbon felt electrodes in vanadium redox flow battery. *J. Power Sources* **2014**, *245*, 66–75. [CrossRef]
4. Ejigu, A.; Edwards, M.; Walsh, D.A. Synergistic Catalyst–Support Interactions in a Graphene–$Mn_3O_4$ Electrocatalyst for Vanadium Redox Flow Batteries. *ACS Catal.* **2015**, *5*, 7122–7130. [CrossRef]
5. Lourenssen, K.; Williams, J.; Ahmadpour, F.; Clemmer, R.; Tasnim, S. Vanadium redox flow batteries: A comprehensive review. *J. Energy Storage* **2019**, *25*, 100844. [CrossRef]
6. Choi, C.; Kim, S.; Kim, R.; Choi, Y.; Kim, S.; Jung, H.-Y.; Yang, J.H.; Kim, H.-T. A review of vanadium electrolytes for vanadium redox flow batteries. *Renew. Sustain. Energy Rev.* **2017**, *69*, 263–274. [CrossRef]
7. Hammer, E.-M.; Berger, B.; Komsiyska, L. Improvement of the performance of graphite felt electrodes for vanadium-redox-flow-batteries by plasma treatment. *Int. J. Renew. Energy Dev.* **2014**, *3*, 7. [CrossRef]
8. Ulaganathan, M.; Aravindan, V.; Yan, Q.; Madhavi, S.; Skyllas-Kazacos, M.; Lim, T.M. Recent advancements in all-vanadium redox flow batteries. *Adv. Mater. Interfaces* **2016**, *3*, 1500309. [CrossRef]
9. Wei, L.; Zhao, T.; Zhao, G.; An, L.; Zeng, L. A high-performance carbon nanoparticle-decorated graphite felt electrode for vanadium redox flow batteries. *Appl. Energy* **2016**, *176*, 74–79. [CrossRef]
10. Yue, L.; Li, W.; Sun, F.; Zhao, L.; Xing, L. Highly hydroxylated carbon fibres as electrode materials of all-vanadium redox flow battery. *Carbon* **2010**, *48*, 3079–3090. [CrossRef]
11. Bayeh, A.W.; Kabtamu, D.M.; Chang, Y.-C.; Wondimu, T.H.; Huang, H.-C.; Wang, C.-H. Carbon and metal-based catalysts for vanadium redox flow batteries: A perspective and review of recent progress. *Sustain. Energy Fuels* **2021**, *5*, 1668–1707. [CrossRef]
12. Cloke, P.L.; Kelly, W.C. Solubility of gold under inorganic supergene conditions. *Econ. Geol.* **1964**, *59*, 259–270. [CrossRef]
13. Lee, W.; Jo, C.; Youk, S.; Shin, H.Y.; Lee, J.; Chung, Y.; Kwon, Y. Mesoporous tungsten oxynitride as electrocatalyst for promoting redox reactions of vanadium redox couple and performance of vanadium redox flow battery. *Appl. Surf. Sci.* **2018**, *429*, 187–195. [CrossRef]
14. Duan, X.; O'Donnell, K.; Sun, H.; Wang, Y.; Wang, S. Sulfur and nitrogen co-doped graphene for metal-free catalytic oxidation reactions. *Small* **2015**, *11*, 3036–3044. [CrossRef]
15. Lee, H.J.; Kim, H. Graphite felt coated with dopamine-derived nitrogen-doped carbon as a positive electrode for a vanadium redox flow battery. *J. Electrochem. Soc.* **2015**, *162*, A1675. [CrossRef]
16. Wei, G.; Jing, M.; Fan, X.; Liu, J.; Yan, C. A new electrocatalyst and its application method for vanadium redox flow battery. *J. Power Sources* **2015**, *287*, 81–86. [CrossRef]
17. Youn, C.; Song, S.A.; Kim, K.; Woo, J.Y.; Chang, Y.-W.; Lim, S.N. Effect of nitrogen functionalization of graphite felt electrode by ultrasonication on the electrochemical performance of vanadium redox flow battery. *Mater. Chem. Phys.* **2019**, *237*, 121873. [CrossRef]
18. Li, Q.; Bai, A.; Zhang, T.; Li, S.; Sun, H. Dopamine-derived nitrogen-doped carboxyl multiwalled carbon nanotube-modified graphite felt with improved electrochemical activity for vanadium redox flow batteries. *R. Soc. Open Sci.* **2020**, *7*, 200402. [CrossRef]
19. Ji, Y.; Li, J.L.; Li, S.F.Y. Synergistic effect of the bifunctional polydopamine–$Mn_3O_4$ composite electrocatalyst for vanadium redox flow batteries. *J. Mater. Chem. A* **2017**, *5*, 15154–15166. [CrossRef]
20. Kuo, Y.-L.; Kencana, S.D.; Su, Y.-M.; Huang, H.-T. Tailoring the $O_2$ reduction activity on hydrangea-like $La_{0.5}Sr_{0.5}MnO_3$ cathode film fabricated via atmospheric pressure plasma jet process. *Ceram. Int.* **2018**, *44*, 7349–7356. [CrossRef]

21. Wang, F.-M.; Kuo, Y.-L.; Huang, L.-S.; Ramar, A.; Su, C.-H. Fabrication of in operando, self-growing, core-shell solid electrolyte interphase on LiFePO$_4$ electrodes for preventing undesirable high-temperature effects in Li-ion batteries. *Electrochim. Acta* **2018**, *268*, 260–267. [CrossRef]

22. Grill, A. *Cold Plasma in Materials Fabrication: From Fundamentals to Applications*; The Institute of Electrical and Electronics Engineers, Inc.: New York, NY, USA, 1994; pp. 46–85.

23. Harry, J.E. Elastic and inelastic collision processes in weakly ionized gases. In *Introduction to Plasma Technology*; Wiley-VCH Verlag & Co. KGaA: Weinheim, Germany, 2010; pp. 15–27.

24. Nist Atomic Spectra Database. Available online: https://www.nist.gov/pml/atomic-spectra-database (accessed on 12 May 2014).

25. Jiang, H.; Shyy, W.; Wu, M.; Zhang, R.; Zhao, T. A bi-porous graphite felt electrode with enhanced surface area and catalytic activity for vanadium redox flow batteries. *Appl. Energy* **2019**, *233*, 105–113. [CrossRef]

26. Wu, L.; Shen, Y.; Yu, L.; Xi, J.; Qiu, X. Boosting vanadium flow battery performance by nitrogen-doped carbon nanospheres electrocatalyst. *Nano Energy* **2016**, *28*, 19–28. [CrossRef]

27. Chang, Y.-C.; Chen, J.-Y.; Kabtamu, D.M.; Lin, G.-Y.; Hsu, N.-Y.; Chou, Y.-S.; Wei, H.-J.; Wang, C.-H. High efficiency of CO$_2$-activated graphite felt as electrode for vanadium redox flow battery application. *J. Power Sources* **2017**, *364*, 1–8. [CrossRef]

28. Kear, G.; Shah, A.A.; Walsh, F.C. Development of the all-vanadium redox flow battery for energy storage: A review of technological, financial and policy aspects. *Int. J. Energy Res.* **2012**, *36*, 1105–1120. [CrossRef]

29. Lee, W.-J.; Wu, Y.-T.; Liao, Y.-W.; Liu, Y.-T. Graphite felt modified by atomic layer deposition with TiO$_2$ nanocoating exhibits super-hydrophilicity, low charge-transform resistance, and high electrochemical activity. *Nanomaterials* **2020**, *10*, 1710. [CrossRef]

30. Li, B.; Gu, M.; Nie, Z.; Wei, X.; Wang, C.; Sprenkle, V.; Wang, W. Nanorod niobium oxide as powerful catalysts for an all vanadium redox flow battery. *Nano Lett.* **2014**, *14*, 158–165. [CrossRef] [PubMed]

31. Shah, A.; Al-Fetlawi, H.; Walsh, F. Dynamic modelling of hydrogen evolution effects in the all-vanadium redox flow battery. *Electrochim. Acta* **2010**, *55*, 1125–1139. [CrossRef]

32. Etesami, M.; Abouzari-Lotf, E.; Ripin, A.; Nasef, M.M.; Ting, T.M.; Saharkhiz, A.; Ahmad, A. Phosphonated graphene oxide with high electrocatalytic performance for vanadium redox flow battery. *Int. J. Hydrog. Energy* **2018**, *43*, 189–197. [CrossRef]

33. Karikalan, N.; Elavarasan, M.; Yang, T.C. Effect of cavitation erosion in the sonochemical exfoliation of activated graphite for electrocatalysis of acebutolol. *Ultrason. Sonochem.* **2019**, *56*, 297–304. [CrossRef]

34. Jiang, H.; Shyy, W.; Wu, M.; Wei, L.; Zhao, T. Highly active, bi-functional and metal-free B$_4$C-nanoparticle-modified graphite felt electrodes for vanadium redox flow batteries. *J. Power Sources* **2017**, *365*, 34–42. [CrossRef]

35. Ciubuc, J.D.; Qiu, C.; Bennet, K.E.; Alonzo, M.; Durrer, W.; Manciu, F.S. Raman computational and experimental studies of dopamine molecules on silver nanocolloids. In Proceedings of the 2017 IEEE International Symposium on Medical Measurements and Applications (MeMeA), Rochester, MN, USA, 7–10 May 2017; pp. 153–158.

36. He, B.; Li, G.; Chen, L.; Chen, Z.; Jing, M.; Zhou, M.; Zhou, N.; Zeng, J.; Hou, Z. A facile N doping strategy to prepare mass-produced pyrrolic N-enriched carbon fibers with enhanced lithium storage properties. *Electrochim. Acta* **2018**, *278*, 106–113. [CrossRef]

37. Kabtamu, D.M.; Chen, J.-Y.; Chang, Y.-C.; Wang, C.-H. Electrocatalytic activity of Nb-doped hexagonal WO$_3$ nanowire-modified graphite felt as a positive electrode for vanadium redox flow batteries. *J. Mater. Chem. A* **2016**, *4*, 11472–11480. [CrossRef]

38. Shao, Y.; Cheng, Y.; Duan, W.; Wang, W.; Lin, Y.; Wang, Y.; Liu, J. Nanostructured electrocatalysts for PEM fuel cells and redox flow batteries: A selected review. *ACS Catal.* **2015**, *5*, 7288–7298. [CrossRef]

39. Ghimire, P.C.; Schweiss, R.; Scherer, G.G.; Wai, N.; Lim, T.M.; Bhattarai, A.; Nguyen, T.D.; Yan, Q. Titanium carbide-decorated graphite felt as high performance negative electrode in vanadium redox flow batteries. *J. Mater. Chem. A* **2018**, *6*, 6625–6632. [CrossRef]

40. Kim, K.J.; Lee, S.-W.; Yim, T.; Kim, J.-G.; Choi, J.W.; Kim, J.H.; Park, M.-S.; Kim, Y.-J. A new strategy for integrating abundant oxygen functional groups into carbon felt electrode for vanadium redox flow batteries. *Sci. Rep.* **2014**, *4*, 1–6. [CrossRef]

41. Bayeh, A.W.; Kabtamu, D.M.; Chang, Y.-C.; Chen, G.-C.; Chen, H.-Y.; Lin, G.-Y.; Liu, T.-R.; Wondimu, T.H.; Wang, K.-C.; Wang, C.-H. Synergistic effects of a TiNb$_2$O$_7$–reduced graphene oxide nanocomposite electrocatalyst for high-performance all-vanadium redox flow batteries. *J. Mater. Chem. A* **2018**, *6*, 13908–13917. [CrossRef]

42. Kwon, O.-J.; Myung, S.-W.; Lee, C.-S.; Choi, H.-S. Comparison of the surface characteristics of polypropylene films treated by Ar and mixed gas (Ar/O$_2$) atmospheric pressure plasma. *J. Colloid Interface Sci.* **2006**, *295*, 409–416. [CrossRef] [PubMed]

43. Wang, R.; Shen, Y.; Zhang, C.; Yan, P.; Shao, T. Comparison between helium and argon plasma jets on improving the hydrophilic property of PMMA surface. *Appl. Surf. Sci.* **2016**, *367*, 401–406. [CrossRef]

44. Deng, F.; Zhang, Y.; Li, X.; Liu, Y.; Shi, Z.; Wang, Y. Synthesis and mechanical properties of dopamine modified titanium dioxide/waterborne polyurethane composites. *Polym. Compos.* **2019**, *40*, 328–336. [CrossRef]

45. Hofman, A.H.; van Hees, I.A.; Yang, J.; Kamperman, M. Bioinspired underwater adhesives by using the supramolecular toolbox. *Adv. Biomater.* **2018**, *30*, 1704640. [CrossRef] [PubMed]

46. Sun, C.; Min, J.; Lin, J.; Wan, H. Effect of atmospheric pressure plasma treatment on adhesive bonding of carbon fiber reinforced polymer. *Polymers* **2019**, *11*, 139. [CrossRef] [PubMed]

47. Zhou, N.; Wang, N.; Wu, Z.; Li, L. Probing active sites on metal-free, nitrogen-doped carbons for oxygen electroreduction: A review. *Catalysts* **2018**, *8*, 509. [CrossRef]

48.  Khan, A.; Jawaid, M.; Khan, A.A.P.; Asiri, A.M. *Electrically Conductive Polymers and Polymer Composites: From Synthesis to Biomedical Applications*; John Wiley & Sons: Hoboken, NJ, USA, 2018.

49.  Tseng, T.-M.; Huang, R.-H.; Huang, C.-Y.; Hsueh, K.-L.; Shieu, F.-S. A Kinetic Study of the Platinum/Carbon Anode Catalyst for Vanadium Redox Flow Battery. *J. Electrochem. Soc.* **2013**, *160*, A690. [CrossRef]

50.  Huang, R.-H.; Sun, C.-H.; Tseng, T.-m.; Chao, W.-K.; Hsueh, K.-L.; Shieu, F.-S. Investigation of active electrodes modified with platinum/multiwalled carbon nanotube for vanadium redox flow battery. *J. Electrochem. Soc.* **2012**, *159*, A1579. [CrossRef]

51.  Jeong, S.; Kim, S.; Kwon, Y. Performance enhancement in vanadium redox flow battery using platinum-based electrocatalyst synthesized by polyol process. *Electrochim. Acta* **2013**, *114*, 439–447. [CrossRef]

52.  Wang, W.; Wang, X. Investigation of Ir-modified carbon felt as the positive electrode of an all-vanadium redox flow battery. *Electrochim. Acta* **2007**, *52*, 6755–6762. [CrossRef]

53.  Kim, K.J.; Park, M.-S.; Kim, J.-H.; Hwang, U.; Lee, N.J.; Jeong, G.; Kim, Y.-J. Novel catalytic effects of $Mn_3O_4$ for all vanadium redox flow batteries. *Chem. Commun.* **2012**, *48*, 5455–5457. [CrossRef] [PubMed]

54.  Pham, H.T.T.; Jo, C.; Lee, J.; Kwon, Y. $MoO_2$ nanocrystals interconnected on mesocellular carbon foam as a powerful catalyst for vanadium redox flow battery. *RSC Adv.* **2016**, *6*, 17574–17582. [CrossRef]